Sustainable Environment Research

RESEARCH

Open Access

Emission characterizations and environmental impacts of off-road vehicles

Hsing-Wang Li[1], Chia-Hsiang Lai[2], Ku-Fan Chen[3], Yi-Ching Lin[4], Po-Yen Chien[4], Wei-Hsiang Chen[4,5], Kang-Shin Chen[4] and Yen-Ping Peng[4,5*]

Abstract

This study measured particulate matter (PM) and gaseous pollutants in the exhaust of off-road vehicles (excavators, bulldozers) during idling and working. The fingerprint of metals in PM and the emission factors of off-road vehicles were investigated. The concentrations of total PM (TPM), PM_{10}, and $PM_{2.5}$ were 14–251, 12–181, and 10–163 mg m^{-3}, respectively, for two kinds of off-road vehicles. PM_{10} occupied 60–70% of TPM, while $PM_{2.5}$ accounted for 80–90%of PM_{10}. The calculated emission factors were 0.64–0.94, 0.53–0.79, and 0.32–0.49 g BHP^{-1} h^{-1} for TPM, PM_{10}, and $PM_{2.5}$, respectively. Metallic elements of PM were analyzed in order to evaluate the carcinogenic and non-carcinogenic risks. The results showed that the emission of total metallic elements from the excavator and two bulldozers are 2.7 and 7.9–22.6 mg m^{-3}, respectively, and the dominant components are Zn, Fe, and Al. The total carcinogenic risk of Cd and Pb decreased from 9.4×10^{-8} to 1.3×10^{-8} with increasing the distance from 0 to 150 m away from the three off-road vehicles (one excavator, and two bulldozers). The non-carcinogenic risk of both Cd and Pb is lower than the limits (hazard index = 1), which is considered acceptable.

Keywords Metals, Off-road vehicles, $PM_{2.5}$, Risk assessment

1 Introduction

The number of off-road vehicles, including aircraft, marine vessels, cars, trucks, and construction machinery, has increased worldwide due to economic development. Emissions such as particulate matter (PM), carbon oxide (CO), carbon dioxide, hydrocarbons, nitrogen oxides (NOx) and sulphur dioxide (SO_2) from non-road mobile machinery contribute considerably to total emissions released into the air [1]. It is reported that 758 kt of NOx (9.4% of the total 8047 kt), 50 kt of $PM_{2.5}$ (3.8% of the total 1321 kt) and 29.2 kt of black carbon (13.4% of the total 218 kt) were attributed to this category for the EU-27 block and Great Britain in 2015 [2]. In addition, PM is also emitted from stationary and mobile sources and has caused severe air pollution in urban areas [3]. The construction equipment was the largest off-road diesel vehicle emission source [4]. With locomotive and marine vessel emissions excluded, off-road diesel equipment accounts for 42% of mobile source exhaust PM_{10} emissions [5]. PM_{10} emitted from construction equipment accounted for 26.5% of the total emissions from off-road vehicles [6]. Besides, excavators were the dominant PM emissions from the construction equipment [7].

PM originating from mobile sources has been linked to several adverse health impacts, including cardiovascular diseases [8]. In addition, fine PM can enter the human

*Correspondence:
Yen-Ping Peng
yppeng@mail.nsysu.edu.tw
[1] Green Energy & System Integration Research & Development Department, China Steel Corporation, Kaohsiung 81233, Taiwan
[2] Department of Biotechnology, National Formosa University, Yunlin 63230, Taiwan
[3] Department of Civil Engineering, National Chi Nan University, Puli 54530, Taiwan
[4] Institute of Environmental Engineering, National Sun Yat-sen University, Kaohsiung 80420, Taiwan
[5] Aerosol Science and Research Center, National Sun Yat-sen University, Kaohsiung 80420, Taiwan

respiratory system, therefore, increasing the incidence of acute and/or chronic health issues [9]. Yu et al. [10] found that $PM_{2.5}$ emissions of non-road construction equipment were majorly composed of carbonaceous components. These carbonaceous particulates and polycyclic aromatic hydrocarbons components represent a particular health risk to the human respiratory system. Epidemiological studies reported that all fractions of PM in children showed significant positive associations with asthma admissions [11]. If it is assumed that 100% of the deposited dose (respiratory tract region surface area per minute) is available for absorption into the systemic circulation, this may lead to overestimate the dose to the target tissue. US Environmental Protection Agency (EPA) suggested that inhalation unit risk and reference concentration for an inhaled chemical contaminant should be considered in inhalation health risk assessment [12].

Atmospheric stability plays an important role in the dispersion of pollutants. The stability of the atmosphere within the planetary boundary layer largely determines the intensity of turbulence and, subsequently, the diffusion processes, which affect pollutants released into this layer. A method for estimating atmospheric stability, incorporating considerations of both mechanical and buoyant turbulence was proposed [13]. The amount of atmospheric turbulence is present in six stability classes, A, B, C, D, E, and F. The classes A, B, and C stand for very unstable, unstable, and slightly unstable conditions, respectively; D stands for a neutral condition; and E and F stand for stable and very stable conditions, respectively [14]. Ruttanawongchai et al. [15] reported that both $PM_{2.5}$ and PM_{10} concentrations were over the standard, slightly stable atmospheres occurred as indicated by the E-class stability plot. In addition, the slightly stable and neutral atmosphere (class E and D, respectively) in Chiang Mai that lasted for about 24 h also contributed to the excess of PM_{10} and $PM_{2.5}$ along with low wind speed.

The Industrial Source Complex Short Term (ISCST) model is a steady-state Gaussian plume model, which can be used to estimate the pollutant concentration from different sources associated with an industrial complex [16]. The ISCST atmospheric dispersion model was used to predict a point source emission, considering one year of hourly meteorological data. The efficiency of the network design increases with the number of samplers, ranging from 0.09 to 0.48 [17]. The ISCST mode also has been applied to assess the possible sites with maximum dioxin concentration in certain region [18]. The other model "the air pollution model (TAPM)" is also commonly used to estimate the distribution of air pollutant. It is a three-dimensional, prognostic, Eulerian, incompressible, non-hydrostatic, primitive equation model [19]. TAPM can predict different pollutant concentrations, such as non-reactive (tracer) and reactive pollutants (e.g., nitrogen dioxide, and particulate) from a variety of sources (e.g., industrial stacks) [20]. Hurley et al. [21] applied TAPM to predict year-long extreme concentration statistics of 24-h averaged particles (PM_{10} and $PM_{2.5}$) across all monitoring sites to within 13%. TAPM predicted the mean and extreme values of the SO_2 in the simulated domain, while the statistical measures showed fair agreement [22]. Previous study reported that point-source emissions were the predominant contributors (about 49.1%) to PM_{10} concentrations at Hsiung-Kong industrial site in Kaohsiung City, followed by area sources (approximately 35.0%) and transport from neighboring areas (7.8%) [23]. In New Zealand, the measured annual mean for PM_{10} is 22 μg m^{-3} as opposed to 18 μg m^{-3} simulated by TAPM. The simulated dispersion of PM_{10} is in good agreement with observed values at a permanent monitoring station [24]. In addition, TAPM model showed some good results in simulating the CO concentrations during winter season when a well-defined boundary layer exists over Bangkok [25]. TAPM model also simulates human movement and behavioral patterns in order to obtain an accurate estimate of individual exposure to a pollutant [26].

Many studies have been conducted to investigate the NOx and PM associated with off-road vehicle emissions [2–7]. However, the information about the particulate size distribution, metal contents in $PM_{2.5}$ of exhausts as well as emission factors (EFs) of different pollutants is very limited. Therefore, it is necessary to study the chemical composition characteristics and EFs of non-road emission $PM_{2.5}$ under realistic conditions to obtain more accurate carcinogenic risk results. The main objectives of the present study were to investigate the impact of ambient PM emitted from off-road vehicles. The different metallic elements of PMs were measured from different vehicle sources. TAPM model is applied to predict the $PM_{2.5}$ concentration from different scenarios, and model performance was evaluated by comparison with measurement and predicated $PM_{2.5}$ concentration. In addition, the carcinogenic risk and total non-carcinogenic risk from different metallic species are estimated. The results of this study should reveal important knowledge about the PM characteristics emitted from off-road vehicles and will provide useful information for the future control strategy of ambient PMs.

2 Materials and methods

2.1 Target of off-road vehicles

In this study, one excavator (E1) and two bulldozers (B1, B2) were selected as the target of off-road vehicles to realize the gaseous and particulate compositions of the exhausts. They did not install any air pollution control

devices. The detailed information for the selected vehicles is listed in Table 1.

The diesel with a sulfur content of 10 ppm was used for all the tested off-road vehicles.

2.2 Sampling and measurement of particulate and gaseous of off-road vehicles

All test vehicles were located in a construction site. The particle samples were collected isokinetically following the Standard Methods issued by Taiwan Environmental Protection Administration (TEPA: NIEA A101.77 C). The on-line analyzer was set on the off-road vehicles and was connected to the vehicle exhaust by a sampling tube. Particulate and gaseous samples were collected under two conditions: idling and working (digging dirt and pushing dirt). Each condition lasted at least 2–3 h, and the test were repeated 3 times for each off-road vehicle. A Horiba (MEXA 584 L, Japan) device was used to measure the CO, total hydrocarbon (THC), and NO_X of the exhaust of off-road vehicles. The measurement ranges are 0–10.00% vol, 0–5000 ppmv, and 0–4,000 ppmv for CO, NOx, and THC, respectively, while display resolutions are 0.01%, 1.0 ppmv, and 2.0 ppmv sequentially. The Horiba device was calibrated by the zero and span calibration before each measurement. In addition, three different standard gases (CO: 1000 ppmv, NOx: 500 ppmv, CH_4: 500 ppmv) were used to check the accuracy of this analyzer every six months. Turnkey optical particle analysis system (Serial No. T1055/ No. T1049, Australia) was used to detect both condensable and filterable PM and continuously measure environmental TPM, PM_{10}, and $PM_{2.5}$ of the exhaust of off-road vehicles. The measurement size ranges were from 0.1 to 100 μm. The Turnkey optical particle analysis system was calibrated by two instruments (LVS-$PM_{2.5}$, Graseby PM_{10}) and R^2 value was over 0.98. In addition, the exhaust flow velocity was measured by pitot tube. PM samples were collected using a 47 mm-diameter quartz filter with a stack sampling device. The quartz filters were pre- and post-conditioned for at least 24 h before weighing. The metallic composition in PM were investigated.

Table 1 Specifications of tested off-road vehicles

ID	Manufacturers	Powers (kW)	Model years
E1 (Excavator)	Komatsu	68	2005
B1 (Bulldozer)	CASE	37	2013
B2 (Bulldozer)	Komatsu	279	2005

2.3 EFs

The EFs of particulate and gaseous compounds of the exhaust of off-road vehicles are calculated by the following equation.

$$\mathrm{EFs} = \frac{\text{emission concentration} \times \text{emission flow}}{\text{engine power}} \quad (1)$$

2.4 Analyses of metallic elements

The filter was placed in a microwave digestion furnace. The samples were heated at 175 ^{O}C for 10 min, and then 11 metals (such as Zn, Cd, Co, Cr, Cu, Fe, Mn, Ni, Pb, As, and Al) were analyzed by inductively coupled plasmas-optical emission spectrometry (ICP/OES, Perkin Elmer Optima 8000). The method detection limits for Zn, Cd, Co, Cr, Cu, Fe, Mn, Ni, Pb, As, and Al were 13.7, 1.25, 1.69, 1.21, 10.21, 12.47, 1.84, 0.83, 6.04, 10.43, 18.13 μg L^{-1}, respectively.

2.5 The air pollution model

The ISCST model, was used to compute ambient air concentration at specified receptor points. Similar methodology has been widely used to simulate ambient air concentrations at specified receptor points for various sources [18]. The ISCST model was employed to simulate the dispersion of $PM_{2.5}$ of exhaust in order to evaluate the health impact of off-road vehicles,

TAPM was used to simulate mesoscale atmospheric motions with meteorological, geographical, and air pollution components. Details of the governing equations for mass, momentum, energy, potential temperature, and species concentration have been described previously [19, 21]. Five square grids were nested on each horizontal layer that had 25×25 grids with the sizes of 30, 10, 3, 1, and 0.3 km. The vertical domain comprised 25 horizontal layers from altitudes of 10 to 8000 m. An emission inventory was obtained using Taiwan emission data system 10.0, which was issued by TEPA in 2016 (https://air.moenv.gov.tw/EnvTopics/AirQuality_6.aspx). TAPM classifies the surface vegetation into 29 classes. Surface data in the model were obtained using geographical charts that were issued by the Ministry of Interior, Taiwan government, to determine area fractions of land use in each grid. The background concentration of $PM_{2.5}$ was set to 10 μg m^{-3}. Details of all boundary conditions have been described by previous studies [19, 21, 23, 27]. Taichung city, located in central Taiwan with about 2.8 million inhabitants, was chosen as the simulation area. Several industrial parks, such

as Taichung industrial park and central Taiwan science park, are suited in this district.

2.6 Health risk assessment

The risk assessment of inhalation exposure to the metallic elements was calculated according to the US EPA human health risk assessment models [12]. Lifetime Average Daily Dose (LADD) that describes the dose rate averaged over an individual's anticipated lifetime. Average Daily Dose (ADD) refers to the dose rate averaged over a specified exposure interval and expressed as a daily dose on a per unit body weight basis. LADD and ADD are inhaled intakes (mg kg^{-1} d^{-1}) calculated by the following formulas.

$$LADD_{inhalation} = \frac{C_{tw} \times IR_{inhalation} \times AF_{inhalation}}{BW} \times \frac{ED}{AT} \quad (2)$$

$$ADD_{inhalation} = \frac{C_{tw} \times IR_{inhalation} \times AF_{inhalation}}{BW} \times \frac{ED}{AT} \quad (3)$$

Where C_{tw} (mg m^{-3}), $IR_{inhalation}$ (Nm^3 d^{-1}), $AF_{inhalation}$ (%), BW (kg), ED (yr), and AT (yr) are metal concentration, daily breathing volume, adsorption fraction, body weight, exposure duration, average time, respectively. In addition, AT = ED × 365 d × 24 h d^{-1} for non-carcinogens, while AT = 70 year × 365 d × 24 h d^{-1} for carcinogens.

The carcinogenic risk was calculated by incorporating the inhalation exposure and toxicity values as follows.

$$Risk = LADD_{total} \times SF \quad (4)$$

where SF (kg d mg^{-1}) is a cancer slope factor.

The non-carcinogenic risk, expressed as the hazard quotient (HQ), was calculated by comparing the inhalation exposure with the reference dose, as follows.

$$HQ = \frac{ADD}{RfD} \quad (5)$$

where RfD (mg kg^{-1} d^{-1}) is reference dose. When carcinogenic risk exceeds 1×10^{-6}, it indicates a higher chance of developing cancer. The hazard index (HI) is the sum of HQ for toxics that affect the same target organ. The level of HI value > 1.0 indicate that there is a greater chance of non-carcinogenic effects [12].

3 Results and discussions

3.1 Gaseous and particulate emissions from off-road vehicles

The concentrations of CO, NOx, THC, $PM_{2.5}$, PM_{10}, and TPM were monitored for a better understanding of the characteristics of off-road vehicles. The gas pollutant concentrations of THC, NOx, and CO of the three off-road vehicles are shown in Fig. 1. Concentrations of THC, NOx, and CO were 12–87, 110–202, and 110–420 ppmv, respectively, for E1; while the concentrations were 11–40, 155–375, and 210–850 ppm for B1. As to B2, the concentrations of THC, NOx, and CO were 62–1860, 89–1100,

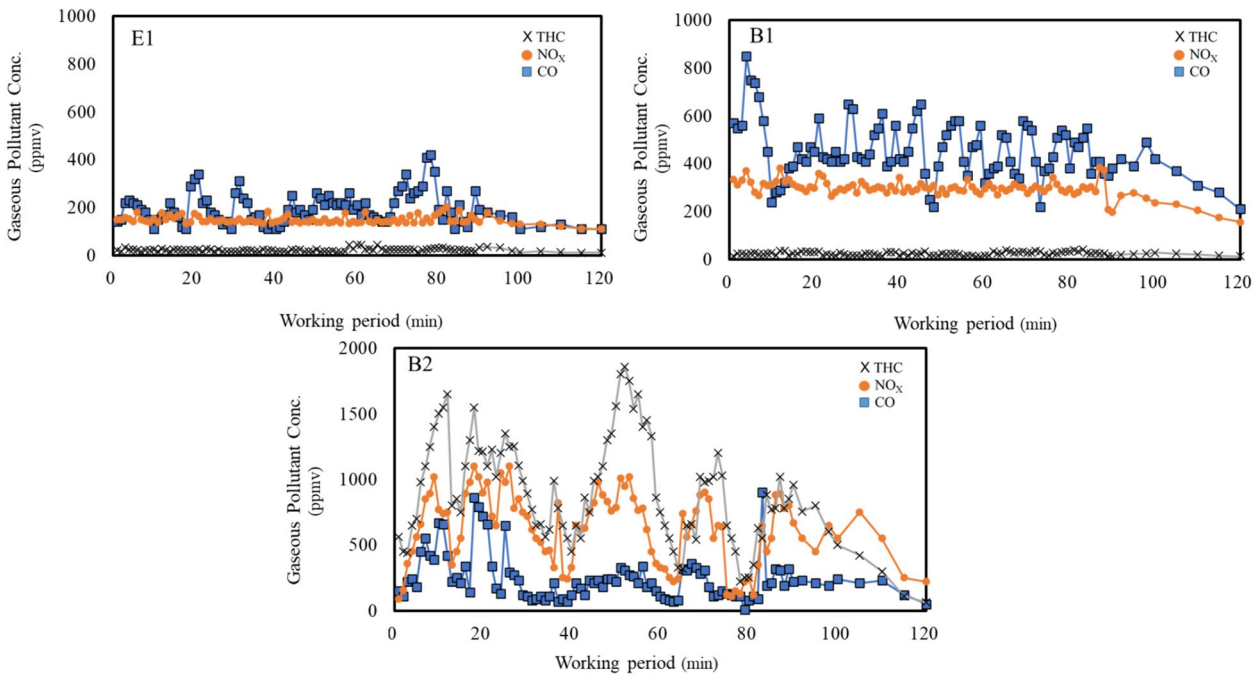

Fig. 1 The gaseous pollutant concentration from different off-road vehicles during the working period

and 9–901 ppmv, individually, which was slightly higher than the E1 and B1 due to the much higher horsepower operation (Table 1). The NOx emission from bulldozers was 89–1100 ppmv which was close to the result of a previous study (202–706 ppmv) [28]. High NOx concentration was found in B2, which may be due to high exhaust gas temperature [29]. CO is emitted during engine start-up and continuous acceleration, and many peaks were found in three vehicles. Much high THC was measured from B2 due to insufficient temperature near the engine cylinder wall [30].

The concentrations of TPM, PM_{10}, and $PM_{2.5}$ emitted from the three off-road vehicles are shown in Fig. 2. Concentrations of TPM, PM_{10}, and $PM_{2.5}$ were 36–193, 17–152 and 14–113 mg m^{-3} for E1; 34–197, 17–163, and 11–102 mg m^{-3} for B1; 14–251, 12–181, 10–148 mg m^{-3} for B2, respectively. In addition, PM_{10} occupied 60–70% of TPM, while $PM_{2.5}$ accounted for 80–90% of $PM_{10,}$ which was similar to the result of a previous report (94%) [31]. Previous study revealed that the coarse particles can come from re-entrained soot and ash particles inside the exhaust channel [32]. The slightly higher PM emissions observed in B2 are attributed to the increased fuel consumed, leading to the enhanced PM emission accordingly [33].

3.2 Metallic elements

The metallic concentrations of the exhaust of off-road vehicles, such as excavators and bulldozers, are listed in Table 2. In the idling condition, the total metallic concentrations were 0.52, 2.11, and 11.2 mg m^{-3} for E1, B1, and B2, respectively. In working conditions, the total metallic concentrations were higher than that of idling at 2.71, 7.92, and 22.6 mg m^{-3} for E1, bulldozer B1, and B2, individually. Those values were similar to the emission concentration of metals (2.1 mg m^{-3}) in diesel engine generators [34]. In addition, the ratio of W/I (working over idling ratio) was 2.0–5.1, indicating higher metallic emissions in working conditions because of higher engine load and more fuel consumption [4]. Furthermore, the higher metallic emissions were measured in B2 than those of E1 and B1 in both idling and working conditions due to the higher off-road vehicle age of B2. The sequence of major species in the idling condition was: Zn (6.88 mg m^{-3}) > Fe (3.83 mg m^{-3}) > Al (0.47 mg m^{-3}), while the sequences were Zn (15.5 mg m^{-3}) > Fe (5.99 mg m^{-3}) > Al (0.89 mg m^{-3}) in the working condition for B2. For E1 in the working condition, the abundant elements in the idling condition were Fe (0.38 mg m^{-3}), Al (0.12 mg m^{-3}), and Mn (0.009 mg m^{-3}), while the Zn (1.10 mg m^{-3}), Al (0.86 mg m^{-3}), Fe (0.72 mg m^{-3}). Regarding the B1, the dominant metals were Fe (1.5 mg m^{-3}), Al (0.43 mg m^{-3}), Mn (0.07 mg m^{-3}), and Pb (0.06 mg m^{-3}) for idling, while the main species were Fe (5.82 mg m^{-3}), Zn (0.97 mg m^{-3}), Al (0.82 mg m^{-3}) and Pb (0.21 mg m^{-3}) in the working condition. Essentially, Zn, Fe, and Al are the dominant elements in those off-road vehicles, which

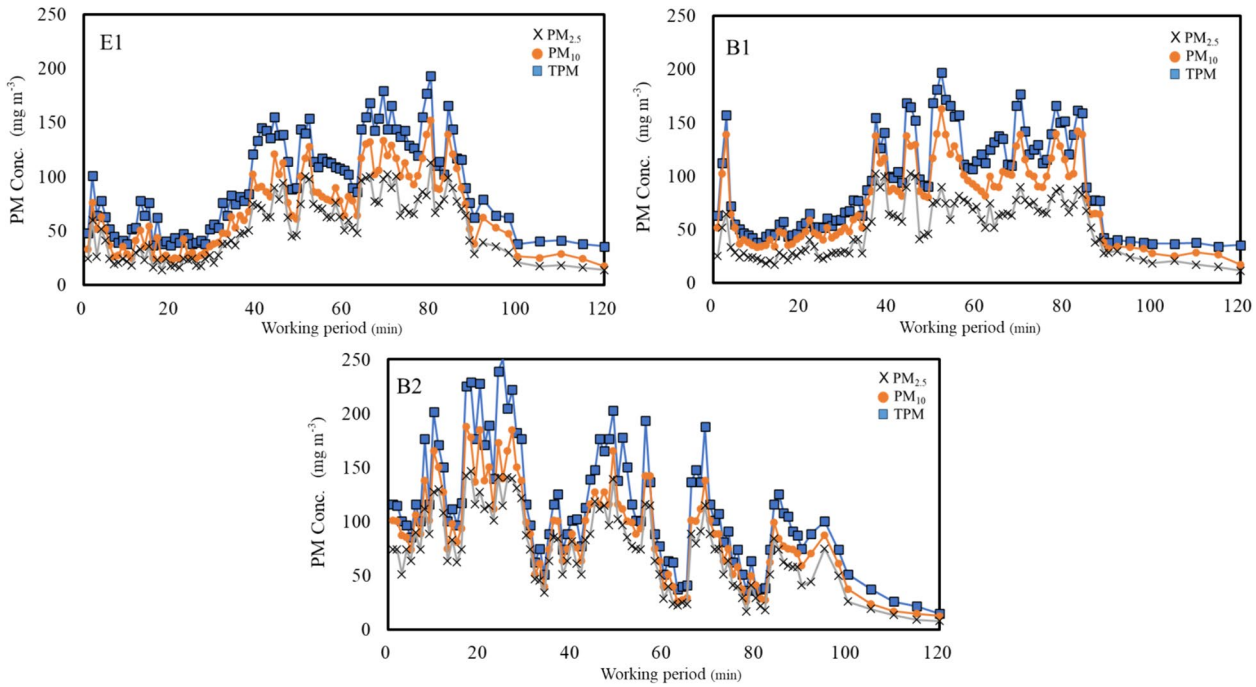

Fig. 2 The particulate matter concentration from different off-road vehicles during the working period

Table 2 The metallic concentrations (mg m^{-3}) from the off-road vehicles at idling and working conditions

Vehicles	E1		B1		B2	
mg m^{-3}	Idling	Working	Idling	Working	Idling	Working
Zn	ND	1.10	ND	0.97	6.88	15.5
Cd	0.001	0.002	0.0005	0.002	0.005	0.001
Co	ND	ND	ND	ND	ND	ND
Cr	ND	ND	0.0005	0.0005	0.009	0.14
Cu	ND	ND	ND	ND	ND	ND
Fe	0.38	0.72	1.55	5.82	3.83	5.99
Mn	0.009	0.01	0.07	0.08	0.05	0.07
Ni	ND	ND	ND	ND	ND	ND
Pb	ND	ND	0.06	0.21	ND	0.11
As	ND	ND	ND	ND	ND	ND
Al	0.12	0.86	0.43	0.83	0.47	0.89
Total	0.52	2.71	2.11	7.92	11.2	22.6
W/I	5.12		3.75		2.01	

is consistent with previous study that Fe was the most abundant element for trucks [4]. Wang et al. [35] also revealed that the concentration of the crustal elements Al, Fe, and Zn accounted for 35% of total elements in diesel fuel. In addition, the Zn element may come from lubricant oil and fuel oil combustion in gasoline and diesel engines [32, 36].

The fraction of metallic elements from three off-road vehicles is shown in Fig. 3. In idling condition, the dominant species were Zn (61%), Fe (34%), and Al (4%) for E1, while the Fe (73–74%), Al (20–23%), and Mn (2–4%) were dominated for B1 and B2. In working conditions, the most abundant elements were Zn (68%), Fe (26%), and Al (4%) for E1, while the proportions of Fe, Zn, and Al accounted for 26–73%, 12–40%, and 10–32%, respectively, for B1 and B2. Cui et al. [4] measured the exhausts for the excavators during 24–42 min sampling time and found that Fe, Zn, and Cu were the most abundant elements.

3.3 EFs

The power-based EFs, expressed as mass rate emitted per brake engine power (g BHP^{-1} h^{-1}), are listed in Table 3. The EFs of CO from three off-road vehicles ranged from 1.8 to 5.8 g BHP $^{-1}$ h^{-1}, which is lower than the emission standard of 10 g BHP $^{-1}$ h^{-1} for diesel and alternative clean fuel engine vehicles. The EFs of NOx ranged from 2.5 to 7.9 g BHP^{-1} h^{-1}, where only the EFs of B1 are slightly higher than the standard of 5.0 g BHP $^{-1}$ h^{-1}. The EFs of HC ranged from 0.13 to 2.9 g BHP $^{-1}$ h^{-1}, where only EFs of B2 are slightly higher than the standard of 1.3 g BHP $^{-1}$ h^{-1}. The EFs of two gas pollutants in this study are similar to the results from nonroad construction equipment of 8.3–13.4, 2.1–16 g BHP $^{-1}$ h^{-1} for NOx, and CO, respectively [37].

The TPM EFs of three off-road vehicles ranged from 0.6 to 0.9 g BHP $^{-1}$ h^{-1}, that are much higher than the diesel and alternative clean fuel engine vehicles standard of 0.1 g BHP $^{-1}$ h^{-1} but lower than the PM EFs (0.4–2.4 g BHP $^{-1}$ h^{-1}) from non-road construction equipment [37]. Notably, the EFs were 0.53–0.79 and 0.32–0.49 g BHP $^{-1}$ h^{-1} for PM_{10} and $PM_{2.5}$, respectively. In general, larger engines, such as the bulldozer, presented higher values of the EFs than the smaller engines. TPM, in particular, has a higher EF. Therefore, future research should focus on emissions of TPM from bulldozers because of its strong link to air quality.

3.4 Simulations of the impact of off-road vehicles on ambient $PM_{2.5}$

ISCST model was used to investigate the impact of emissions of off-road vehicles on atmospheric quality. The calculated $PM_{2.5}$ concentration in different atmospheric stability is listed in Table 4. At atmospheric stability of B-unstable class, the pollutants could transport to a downwind location 270 m away from the pollution source. The $PM_{2.5}$ concentration was calculated as 2.5×10^{-4} μg m^{-3} at 90 m from the source, while the max ground level concentration was 3.2×10^{-4} μg m^{-3}. At atmospheric stability of C-unstable class, the calculated $PM_{2.5}$ concentration was 6.0×10^{-4} μg m^{-3} at 60 m away from the pollution source, while the max ground level concentration was 6.8×10^{-4} μg m^{-3}. At D class with neutral atmospheric condition, the simulated $PM_{2.5}$ concentration was 8.0×10^{-4} μg m^{-3} at 60 m away from the pollution source, while the max ground

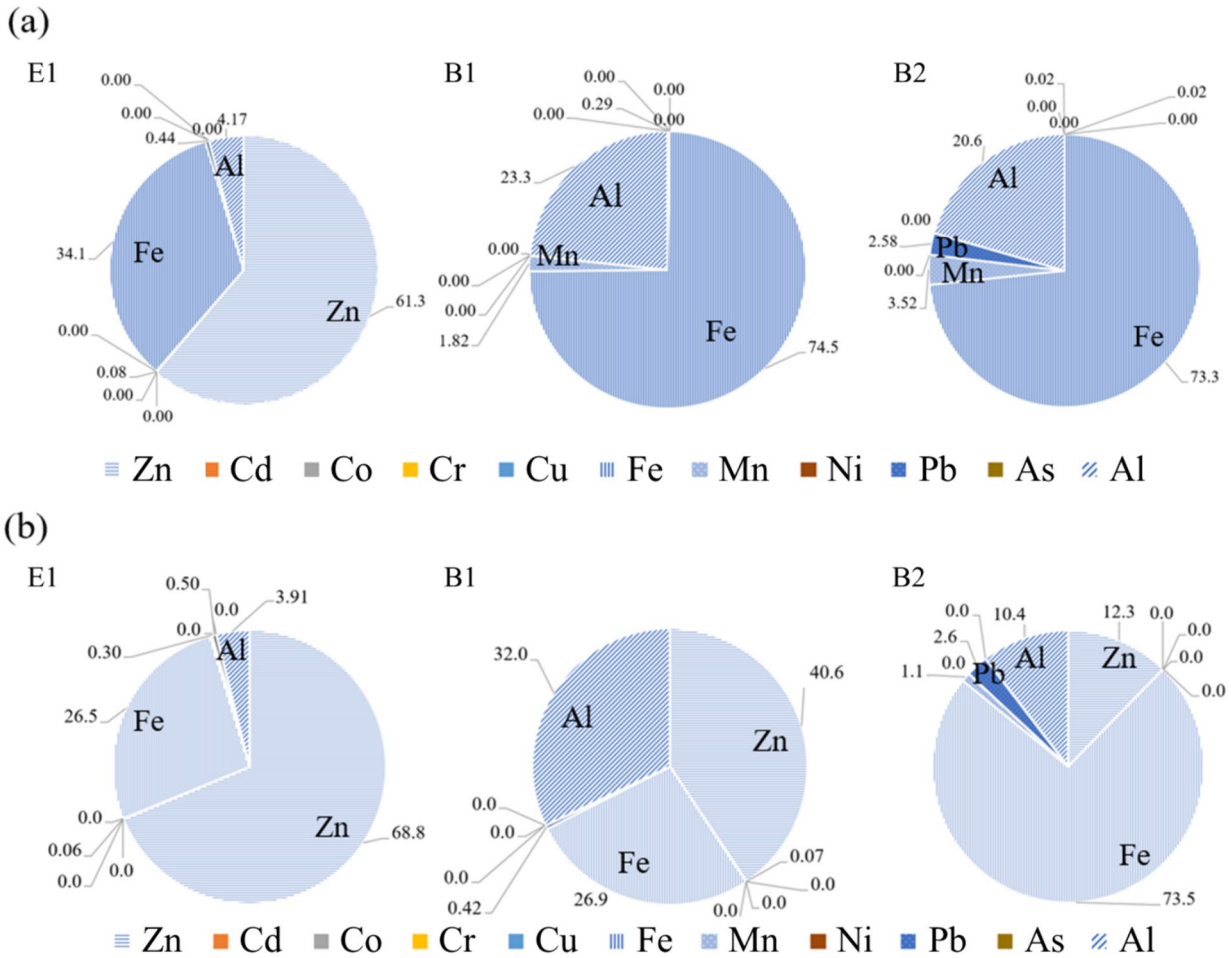

Fig. 3 The fraction of metallic elements at different vehicles **a**: Idling; **b**: Operation

Table 3 The emission factor of gas pollutant and particulate matter from different off-road vehicles during the working

Vehicles g BHP $^{-1}$ h^{-1}	E1	B1	B2	Standard[a]
CO	1.9–4.3 (2.7)	3.5–7.4 (5.8)	0.9–3.1 (1.8)	10
NOx	2.2–2.8 (2.5)	6.8–8.8 (7.9)	2.3–8.1 (4.8)	5.0
THC	0.12–0.14 (0.13)	0.19–0.35 (0.28)	1.8–4.5 (2.9)	1.3
TPM	0.64–0.76 (0.70)	0.82–1.00 (0.94)	0.35–0.97 (0.64)	0.1
PM_{10}	0.49–0.60 (0.54)	0.63–0.81 (0.79)	0.28–0.86 (0.53)	Non
$PM_{2.5}$	0.14–0.37 (0.32)	0.47–0.53 (0.49)	0.22–0.81 (0.46)	Non

[a] Emission Standards for Diesel and Alternative Clean Fuel Engine Vehicles, Ministry of Environment, Taiwan

level concentration reached 1.3×10^{-2} μg m^{-3}. At atmospheric stability of E-stable class, the $PM_{2.5}$ concentration was 9.0×10^{2} μg m^{-3} at 60 m away from sources, and the maximum ground level concentration reached to 1.8×10^{3} μg m^{-3}. According to the above results, atmospheric stability plays an important role in ambient $PM_{2.5}$ concentration. This phenomenon is similar to the higher PM concentrations observed at ground level at nighttime due to less turbulence [15]. Zafra-Mejia et al. [38] also indicated that the PM_{10} concentrations were associated with the highest degree of daytime atmospheric instability. Furthermore, the enhancement of PM concentration

Table 4 The predicted $PM_{2.5}$ concentration (μg m^{-3}) in different atmospheric stability

Atmospheric stability	Max Con.	Con. 60 m	Con. 90 m
B	3.2×10^{-4}		2.5×10^{-4}
C	6.8×10^{-4}	6.0×10^{-4}	
D	1.3×10^{-2}	8×10^{-4}	
E	1.8×10^{3}	9.0×10^{2}	

under stable conditions depends on the distance between the source and the observation point [39]. Zoras et al. [40] illustrated that the PM_{10} worst-case episode is more likely to happen under neutral D to stable atmosphere F at the sampling station.

3.5 Health risk assessment

Health risk assessment of emissions of off-road vehicles was investigated according to previous ISCST results. LADD and ADD from different metals at different downwind locations are listed in Table 5. The highest LADD and ADD were observed in Zn as three off-road vehicles operating simultaneously, followed by Fe, Al, Pb, Mn, Cr, and Cd. The LADD of Zn were 145, 126, 63, and 0 (10^{-6} mg kg^{-1} d^{-1}) from the distance of vehicle sources at 0, 30, 90, and 150 m, respectively, while the ADD of Zn were 290, 252, 63 and 8 (10^{-6} mg kg^{-1} d^{-1}). The LADD and ADD values of other metals also showed that those values decreased with increasing distance from the vehicle sources.

Table 6 lists the carcinogenic and no-carcinogenic risk of Cd and Pb at different downwind locations. The total carcinogenic risk of Cd and Pb decreased from 9.4×10^{-8} to 1.3×10^{-8} with increasing the distances from three off-road vehicles. The most cancer risk was attributed to Pb (> 99.9%). The results showed that the two selected elements had a carcinogenic risk lower than the lifetime cancer risk (1.0×10^{-6}). The total non-carcinogenic risk of Cd and Pb decreased from 3×10^{-5} to 0 by increasing the distances from three off-road vehicles. The results showed that the two selected elements had a non-carcinogenic risk within the limits (HI = 1), which is considered an acceptable risk. Above results revealed that the carcinogenic risk and non-carcinogenic risk from three working vehicles were lower than the threshold, which is no significant health effects on the surrounding residents.

3.6 TAPM simulation for the evaluation of $PM_{2.5}$ contribution from off-road vehicles

TAPM was employed to evaluate the contribution of off-road vehicles to $PM_{2.5}$ concentration. Figure 4 shows the simulated wind vectors and the concentration contours of $PM_{2.5}$ at AM 09:00 and PM 14:00, respectively, on November 29, 2018. The prevailing winds were north and east, with a wind speed of 0.5–1 m s^{-1} at AM 9:00 (Fig. 4a) and 5–6 m s^{-1} at PM 14:00 (Fig. 4b) in the studied domain. Figure 4 also indicates the $PM_{2.5}$ concentration was high (55–82 μg m^{-3}) close to the coastal area, where several industrial processes are located, but was low (11–33 μg m^{-3}) in a mostly rural area. Figure 5 shows the 3-d comparison results between the hourly simulated and measured data of $PM_{2.5}$ concentration. The measured data were obtained from Zhonming station, one of the TEPA monitoring sites. Model performance was evaluated relative to actual measurements using the

Table 5 The LADD and ADD from different metals at different downwind locations

Metals	LADD 0 m	ADD	LADD 30 m	ADD	LADD 90 m	ADD	LADD 150 m	ADD
Zn	145	290	126	252	63	63	0	8
Cd	0.01	0.03	0.11	0.02	0.007	0.01	0	0
Cr	0.13	0.26	0.11	0.22	0.06	0.11	0	0.03
Fe	54	108	47	96	38	37	6	7
Mn	0.76	1.53	0.62	1.26	0.12	0.60	0.03	0.08
Pb	1.89	3.78	1.55	3.09	1.37	1.49	0.03	0.11
Al	7.81	15.60	7.01	14.0	4.35	9.91	0.45	0.91

Unit: 10^{-6} mg kg^{-1} d^{-1}

Table 6 The carcinogenic and non-carcinogenic risk of Cd and Pb at different downwind sites

		0 m	30 m	90 m	150 m
Carcinogenic risk	Cd	6×10^{-12}	5×10^{-12}	2×10^{-12}	6×10^{-13}
	Pb	0.094×10^{-6}	0.085×10^{-6}	0.037×10^{-6}	0.013×10^{-6}
	total	0.094×10^{-6}	0.085×10^{-6}	0.037×10^{-6}	0.013×10^{-6}
Non-carcinogenic risk	Cd	9×10^{-6}	8×10^{-6}	3×10^{-6}	0
	Pb	2.1×10^{-5}	1.9×10^{-5}	1.1×10^{-5}	0
	total	3×10^{-5}	2.7×10^{-5}	1.4×10^{-5}	0

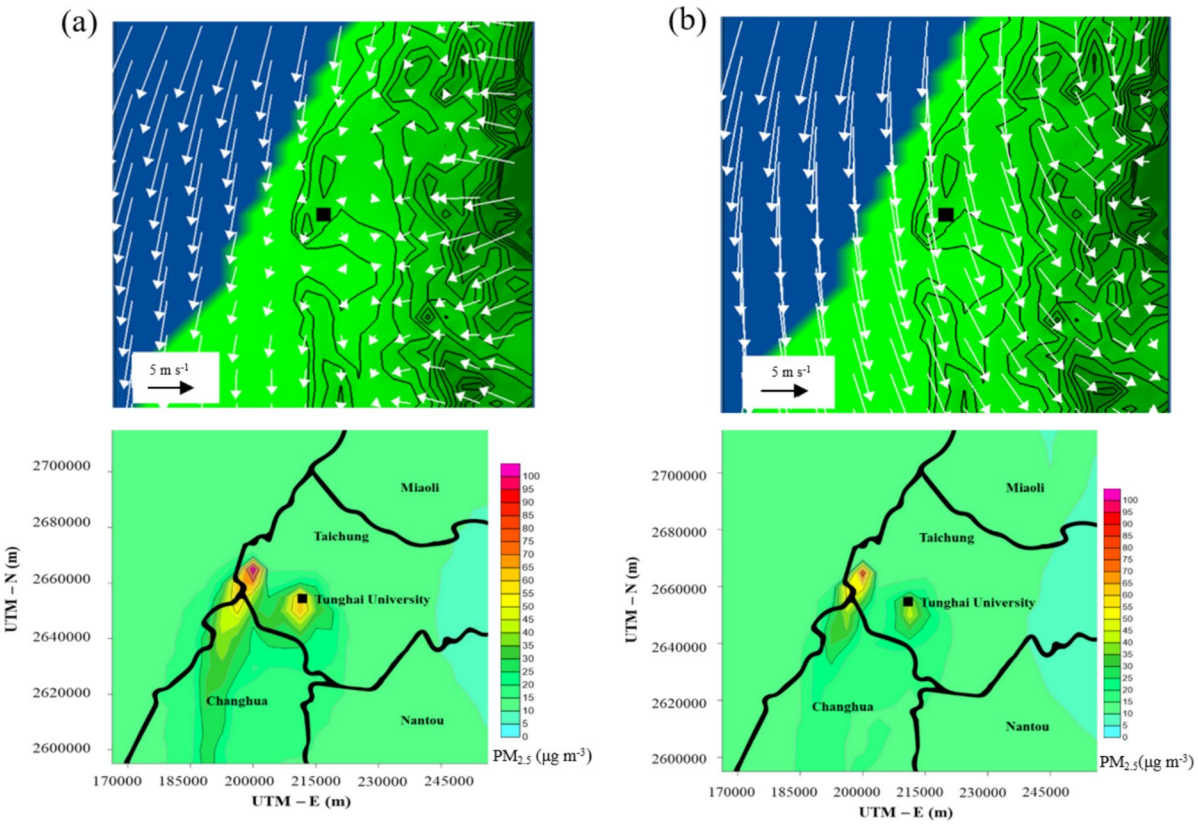

Fig. 4 Simulated surface wind vectors and $PM_{2.5}$ concentration contour (μg m^{-3}) on November 29, 2018, at **a** 09:00 and **b** 14:00

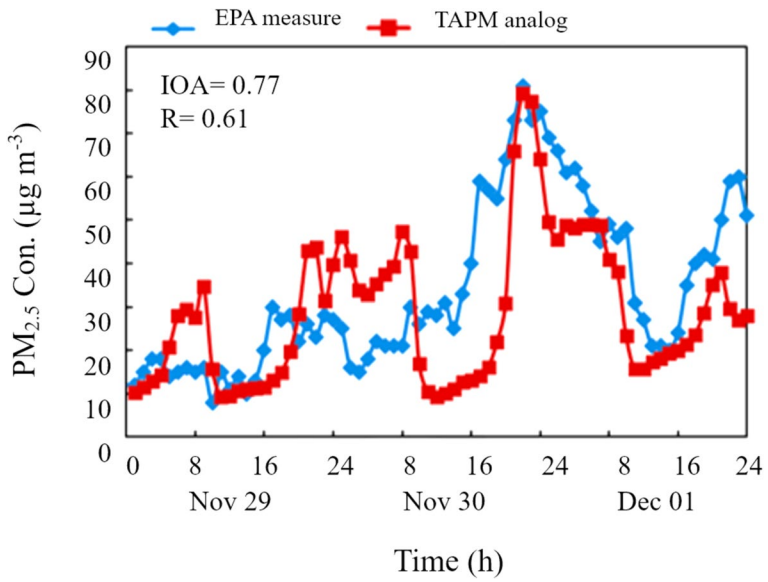

Fig. 5 Comparisons of hourly surface $PM_{2.5}$ concentration at sampling site from November 29 to Dec 1, 2018

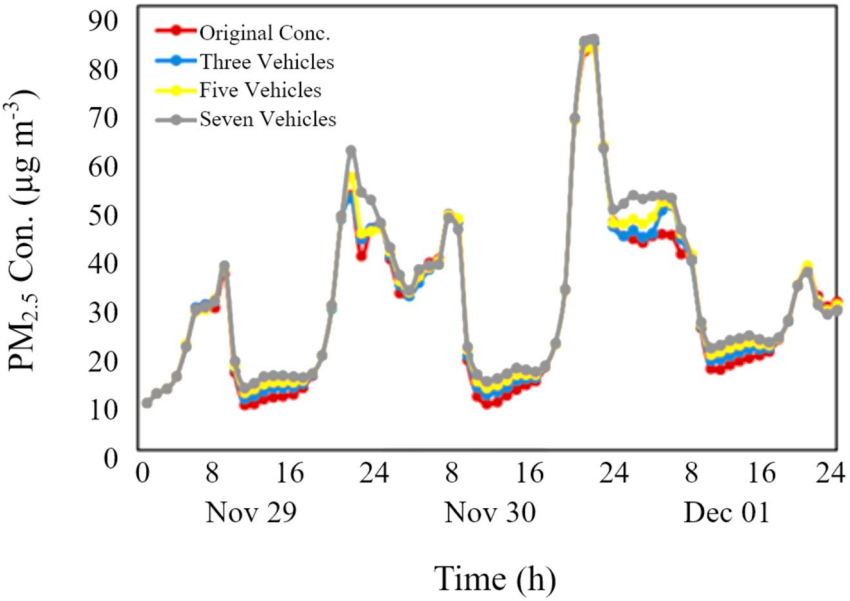

Fig. 6 Comparisons of simulated $PM_{2.5}$ contributed from the exhausts of 3, 5, and 7 off-road vehicles

correlation coefficient (R) and the index of agreement (IOA) [41].

$$\mathrm{IOA} = 1 - \frac{\sum_{i=1}^{N}(|P_i - O_i|)^2}{\sum_{i=1}^{N}\left(|P_i - \overline{O}| + |O_i - \overline{O}|\right)^2} \quad (6)$$

where P_i and O_i are predicted and measured values, respectively, with a sample size *of N*, and $\bar{O}$ is the average of measured data. The simulations generally agree well with the measurements, with a correlation coefficient of $R = 0.61$, and an $IOA = 0.77$. The agreement between prediction and measurement is regarded as good when IOA exceeds 0.5 [19, 21]. Wang et al. [23] applied TAPM to simulate the PM_{10} concentration with $IOA = 0.52–0.76$, indicating a generally good agreement. Figure 6 presents the simulation of the incremental impact of exhausts of off-road vehicles on ambient $PM_{2.5}$ concentration in different scenarios, i.e., three, five, and seven off-road vehicles operated simultaneously for 72 h. Three off-road vehicles resulted in an increase of 22 μg m^{-3} in $PM_{2.5}$, corresponding to an increase of about 1.1%, while five and seven off-road vehicles resulted in an increase of 105 and 177 μg m^{-3} in $PM_{2.5}$, respectively, within 72 h simulated time. The incremental percentages are approximately 5.0% and 8.5%. A previous study reported that in the same lane and street, the average $PM_{2.5}$ concentration during the on-peak period for the number of motor vehicles is approximately 2.2–2.5 and 70–77 times higher than those during the flat peak and low ebb periods, respectively [42]. In addition, $PM_{2.5}$ emission levels of motor vehicles on normal weekdays were overall higher than those on weekends [43].

4 Conclusions

The exhausts of one excavator and two bulldozers were measured to understand the characteristic of the exhausts of off-road vehicles. The gaseous and particulate compounds of the exhaust were analyzed and converted to the emissions factors. Results indicated that both gaseous and particulate compounds increased with an increased horsepower of off-road vehicles. The EFs were 1.8–5.7, 2.5–7.9, and 0.13–2.9 g BHP^{-1} h^{-1} for CO, NOx, and THC, respectively. As to the PM, the EFs were 0.53–0.79 and 0.32–0.49 g BHP^{-1} h^{-1} for PM_{10} and $PM_{2.5}$, respectively. In working conditions, the concentration of total metals from B2 was 22 mg m^{-3}, which was approximately 3–8 times higher than 2.7 to 7.9 mg m^{-3} from E1 and B1. The most abundant elements were Zn (68%), Fe (26%), and Al (4%) from E1, while the proportions of Fe, Zn, and Al were 26–73%, 12–40%, and 10–32%, respectively, from B1 and B2. Two selected elements had a carcinogenic risk lower than lifetime cancer risk (1.0×10^{-6}) and had a non-carcinogenic risk within limits (HI = 1). The results of the risk assessment analysis revealed no significant health effect from three working vehicles on the surrounding residents. According to the TAPM simulation results, seven off-road vehicles operate at the same time, leading to the ambient $PM_{2.5}$ concentration increase by 8.5%.

Acknowledgements
The authors acknowledge Mr. Tzu-Heng Lin and Professor Yu-Min Chang for their help in sampling and analysis work. This work is partially funded by TEPA.

Authors' contributions
All authors contributed equally to this study.

Funding
This study was funded by the Environmental Protection Agency of Taiwan.

Availability of data and materials
The datasets during and/or analyzed during the current study are available from the corresponding author on reasonable request.

Declarations

Competing interests
The authors declare that they have no competing interests.

Received: 31 October 2023 Accepted: 23 April 2024
Published online: 13 June 2024

References

1. Hagan R, Markey E, Clancy J, Keating M, Donnelly A, O'Connor DJ, et al. Non-road mobile machinery emissions and regulations: A review. Air. 2023;1:14–36.
2. CEIP. Data viewer – reported emissions data. Vienna: Centre on Emission Inventories and Projections; 2021.
3. Aggarwal P, Jain S. Impact of air pollutants from surface transport sources on human health: A modeling and epidemiological approach. Environ Int. 2015;83:146–57.
4. Cui M, Chen Y, Feng Y, Li C, Zheng J, Tian C, et al. Measurement of PM and its chemical composition in real-world emissions from non-road and on-road diesel vehicles. Atmos Chem Phys. 2017;17:6779–95.
5. USEPA. National Air Pollutant Emission Trends Update, 1970–1997 [EPA-454/E-98-007]. Washington, DC: United States Environmental Protection Agency; 1998.
6. Zhang LJ, Zheng JY, Yin SS, Peng K, Zhong LJ. Development of non-road mobile source emission inventory for the Pearl River Delta region. Environ Sci (Huan Jing Ke Xue). 2010;31:886–91 [in Chinese].
7. Li DL, Wu Y, Zhou Y, Du X, Fu LX. Fuel consumption and emission inventory of typical construction equipments in China. Environ Sci (Huan Jing Ke Xue). 2012;33:518–24 [in Chinese].
8. Geller MD, Ntziachristos L, Mamakos A, Samaras Z, Schmitz DA, Froines JR, et al. Physicochemical and redox characteristics of particulate matter (PM) emitted from gasoline and diesel passenger cars. Atmos Environ. 2006;40:6988–7004.
9. Turner MC, Krewski D, Pope CA III, Chen Y, Gapstur SM, Thun MJ. Long-term ambient fine particulate matter air pollution and lung cancer in a large cohort of never-smokers. Am J Respir Crit Care Med. 2011;184:1374–81.
10. Yu F, Li C, Liu J, Liao S, Zhu M, Xie Y, et al. Characterization of particulate smoke and the potential chemical fingerprint of non-road construction equipment exhaust emission in China. Sci Total Environ. 2020;723:137967.
11. Tecer LH, Alagha O, Karaca F, Tuncel G, Eldes N. Particulate matter ($PM_{2.5}$, $PM_{10-2.5}$, and PM_{10}) and children's hospital admissions for asthma and respiratory diseases: a bidirectional case-crossover study. J Toxicol Env Heal A. 2008;71:512–20.
12. USEPA. Risk Assessment Guidance for Superfund (RAGS): Part F. Washington, DC: United States Environmental Protection Agency; 2009.
13. Pasquill F. The estimation of the dispersion of windborne material. Meteorol Mag. 1961;90:33–40.
14. Turner DB. Workbook of Atmospheric Dispersion Estimeates. 2nd ed. Boca Raton: CRC Press; 2020.
15. Ruttanawongchai S, Raktham C, Khumsaeng T. The influence of meteorology on ambient $PM_{2.5}$ and PM_{10} concentration in Chiang Mai. J Phys Conf Ser. 2018;1144:012088.
16. USEPA. Air Quality Dispersion Modeling - Alternative Models. Washington, DC: United States Environmental Protection Agency; 2023.
17. Mazzeo NA, Venegas LE. Practical use of the ISCST3 model to select monitoring site locations for air pollution control. Int J Environ Pollut. 2000;14:246–59.
18. Wu YL, Li HW, Chien CH, Lai YC, Wang LC. Monitoring and identification of polychlorinated dibenzo-*p*-dioxins and dibenzofurans in the ambient central Taiwan. Aerosol Air Qual Res. 2010;10:463–71.
19. Hurley P. The Air Pollution Model (TAPM) Version 3. CSIRO Atmospheric Research Technical Papers (No. 71 and 72). Canberra: Commonwealth Scientific and Industrial Research Organisation; 2005.
20. Hurley PJ, Physick WL, Luhar AK. TAPM: a practical approach to prognostic meteorological and air pollution modelling. Environ Modell Softw. 2005;20:737–52.
21. Hurley P, Manins P, Lee S, Boyle R, Ng YL, Dewundege P. Year-long, high-resolution, urban airshed modelling: verification of TAPM predictions of smog and particles in Melbourne, Australia. Atmos Environ. 2003;37:1899–910.
22. Matthaios VN, Triantafyllou AG, Albanis TA, Sakkas V, Garas S. Performance and evaluation of a coupled prognostic model TAPM over a mountainous complex terrain industrial area. Theor Appl Climatol. 2018;132:885–903.
23. Wang WC, Chen KS. Modeling and analysis of source contribution of PM_{10} during severe pollution events in southern Taiwan. Aerosol Air Qual Res. 2008;8:319–38.
24. Zawar-Reza P, Kingham S, Pearce J. Evaluation of a year-long dispersion modelling of PM_{10} using the mesoscale model TAPM for Christchurch, New Zealand. Sci Total Environ. 2005;349:249–59.
25. Jinsart W, Sripraparkorn C, Siems ST, Hurley PJ, Thepanondh S. Application of The Air Pollution Model (TAPM) to the urban airshed of Bangkok, Thailand. Int J Environ Pollut. 2010;42:68–84.
26. Newth D, Gunasekera D. An integrated agent-based framework for assessing air pollution impacts. J Environ Prot. 2012;3:1135–46.
27. Peng YP, Chen KS, Lou JC, Hwang SW, Wang WC, Lai CH, et al. Measurements and mesoscale modeling of autumnal vertical ozone profiles in southern Taiwan. Terr Atmos Ocean Sci. 2008;19:505–14.
28. Tan P, Yao J, Yao C, Hu Z, Lou D, Lu S, et al. Study of real-road nitrogen oxide emissions of non-road vehicles. J Phys Conf Ser. 2022;2160:012050.
29. Youn I, Jeon J. Combustion performance and low NOx emissions of a dimethyl ether compression-ignition engine at high injection pressure and high exhaust gas recirculation rate. Energies. 2022;15:1912.
30. Tutak W, Jamrozik A, Grab-Rogalinski K. The effect of RME-1-butanol blends on combustion, performance and emission of a direct injection diesel engine. Energies. 2021;14:2941.
31. Shen X, Kong L, Shi Y, Cao X, Li X, Wu B, et al. Multi-type air pollutant emission inventory of non-road mobile sources in China for the period 1990–2017. Aerosol Air Qual Res. 2021;21:210003.
32. Moldanova J, Fridell E, Winnes H, Holmin-Fridell S, Boman J, Jedynska A, et al. Physical and chemical characterisation of PM emissions from two ships operating in European Emission Control Areas. Atmos Meas Tech. 2013;6:3577–96.
33. Mohankumar S, Senthilkumar P. Particulate matter formation and its control methodologies for diesel engine: A comprehensive review. Renew Sust Energ Rev. 2017;80:1227–38.
34. Lin SL, Tsai JH, Chen SJ, Huang KL, Lin CC, Huang HT, et al. Emissions of polycyclic aromatic hydrocarbons and particle-bound metals from a diesel engine generator fueled with waste cooking oil-based biodiesel blends. Aerosol Air Qual Res. 2017;17:1679–89.
35. Wang YF, Huang KL, Li CT, Mi HH, Luo JH, Tsai PJ. Emissions of fuel metals content from a diesel vehicle engine. Atmos Environ. 2003;37:4637–43.
36. Lin YC, Tsai CJ, Wu YC, Zhang R, Chi KH, Huang YT, et al. Characteristics of trace metals in traffic-derived particles in Hsuehshan Tunnel, Taiwan: size distribution, potential source, and fingerprinting metal ratio. Atmos Chem Phys. 2015;15:4117–30.
37. Zhu D, Nussbaum NJ, Kuhns HD, Chang MCO, Sodeman D, Moosmuller H, et al. Real-world PM, NO_x, CO, and ultrafine particle emission factors for military non-road heavy duty diesel vehicles. Atmos Environ. 2011;45:2603–9.
38. Zafra-Mejia CA, Rodriguez-Miranda JP, Rondon-Quintana HA. The relationship between atmospheric condition and human mortality associated with coarse material particulate in Bogotá (Colombia). Rev Logos Cienc Tecnol. 2020;12:57–68 [in Portuguese].

39. Lott RA. Case study of plume dispersion over elevated terrain. Atmos Environ. 1984;18:125–34.
40. Zoras S, Triantafyllou AG, Deligiorgi D. Atmospheric stability and PM10 concentrations at far distance from elevated point sources in complex terrain: Worst-case episode study. J Environ Manage. 2006;80:295–302.
41. Willmott CJ, Ackleson SG, Davis RE, Feddema JJ, Klink KM, Legates DR, et al. Statistics for the evaluation and comparison of models. J Geophys Res-Oceans. 1985;90:8995–9005.
42. Wang B, Li Y, Tang Z, Cai N, Niu H. Effects of vehicle emissions on the $PM_{2.5}$ dispersion and intake fraction in urban street canyons. J Clean Prod. 2021;324:129212.
43. Tong R, Liu J, Wang W, Fang Y. Health effects of $PM_{2.5}$ emissions from on-road vehicles during weekdays and weekends in Beijing, China. Atmos Environ. 2020;223:117258.

Publisher's Note